Non-linear Contact Analysis and Response Surface Optimization of Railway Wheel Using ANSYS

Abhishek Agarwal[1*] , Ambika Rimal[1] , Masengo Ilunga[2]

[1] Department of Mechanical Engineering, College of Science & Technology, Royal University of Bhutan, Phuentsholing 21101, Bhutan
[2] Department of Civil Engineering, University of South Africa, Pretoria 1709, South Africa

Corresponding Author Email: agarwala.cst@rub.edu.bt

ABSTRACT

The onset and propagation of fractures significantly impact the remaining operational lifespan of locomotive wheels and rail infrastructure, primarily influenced by contact stresses arising from their interaction. This study employs the nonlinear Newton-Raphson algorithm to comprehensively evaluate the structural characteristics and critical regions of the rail-wheel contact-zone. The rail wheel CAD model is developed in the ANSYS-Design_Modeler, and then it undergoes a static structural analysis using its system for this purpose. A comparative analysis between linear and nonlinear approaches through simulation indicates a consistent overestimation of contact parameters–penetration, and frictional stress. In particular, the linear performance analysis shows a penetration value 25 percent lower and frictional stress 6.38 percent less than that of the nonlinear response. This study highlights the importance of nonlinear analysis when it comes to capturing the subtle complexities inherent in actual wheel-rail interactions and reveals the shortcomings of linear analysis in giving correct predictions. The optimization process is conducted on a railway locomotive wheel using the optimal space-filling algorithm of the response surface optimization process. From the optimization process, the effect of each design variable is evaluated and for most of the structural evaluation parameters, tread_width shows a higher sensitivity percentage and therefore has a higher effect as compared to tread_depth.

1. INTRODUCTION

This scientific study of the mechanisms of wheels-on-rails interaction at high speeds is an important and intricate area for research and innovation, bringing together a vast amount of historical data accumulated over many years of practical practice in running these trains all around our planet. The interaction of high-speed rails and wheels can be analyzed in different distinct domains. The indicated areas include the basic laws governing how wheels and rails interact with each other – contact mechanics, alignment correction of wheel-rail profiles and materials as well as adhesion properties surfaces that come in touch, wear on contact surface webpage rolling fatigue contacts created by tools, noise produced from interaction between completed vehicles. The previous study emphasizes the operational challenges that may involve the wheel-rail rolling contact pair, in a general view of its basic work. Wheel rail separation and collision are weirdly observable as part of rolling contact [1, 2]. This situation may intensify the degradation of wheels and rails, thus promoting injuries [3]. More importantly, it has the capacity to generate a high level of impact noise [4].

Additionally, it has the ability to reduce the level of adherence between the train's wheels and the rails, consequently impacting the train's standard traction and braking performance [5]. Train derailments can occur as a consequence of significant events. Train derailments can occur as a consequence of significant incidents. An ongoing concern among scholars studying railway vehicle dynamics and maintenance engineers specializing in wheel-track repair is the matter of wheel-rail contact. The analysis of the forces exerted between the wheel and the rail is undeniably the most critical factor in studying the dynamic properties of a railway vehicle. The shape of the contact area on the locomotive tire casing exhibits an elliptical geometry. The rail wheel system exhibits an elliptical contact region. Due to the limited contact ellipse area, higher levels of stress will be produced. The Hertz hypothesis proposes the formation of a contact region between two solid materials that are under vertical pressures and compressed against each other. The hypothesis is commonly applied in the analysis of stress distribution in the contact region between a wheel and rail. Both the shape and the contact region of two elastic materials are in a state of static equilibrium.

The microscale examination of the effective contact area to nominal area ratio, as emphasized by Spiryagin et al. [6], underscores the negligible nature of this ratio. Acknowledging the inherent abrasive characteristics of technical surfaces,

especially at the microscale, is critical. To address this, the Gensys railway vehicle multibody software platform has evolved by incorporating an algorithm specifically designed for calculating contact stresses in wheel-rail couplings. This algorithm integrates multiple surface roughness parameters, and tribological characteristics, and considers elastic and plastic deformations, enhancing the precision of contact event replication. The research, employing locomotive multibody simulations, introduces a novel wheel-rail coupling methodology. The study aims to assess the proposed algorithm's viability through comparative analyses with results obtained from original Extended contact wheel-rail couplings, maintaining consistent operational and simulation conditions. Valuable insights into contact stress variations between "ideal" and "rough" conditions (Rail Ra = 0.4 μm and Wheel Ra = 0.7 μm) are gleaned, although certain study constraints are acknowledged.

In contrast, Bernal et al. [7] highlighted the complexity of accurately predicting rail damage due to dynamic conditions resulting from varying speeds and configurations. The paper introduces a system leveraging friction data, digital locomotive replicas, and calibrated shakedown maps to simulate rail surface degradation. Enhanced accuracy in rail damage predictions is achieved through integrating slip-dependent friction characteristics, co-simulating the locomotive traction mechatronic system, and conducting tensile testing. Post-processing techniques transform stress results into calibrated shakedown heatmaps, illustrating the influence of operational conditions on rail deterioration.

Tao et al. [8] delved into locomotive tire wear intricacies, surpassing other rolling stock wear complexities. The simulation model development involves a rolling contact model, a creep control model, and a three-dimensional model. Results reveal the feasibility of representing seismic characteristics, emphasizing the substantial impact of traction, deceleration, and control modes on wheel degradation. The study underscores the effectiveness of a control mode incorporating a programmable creep threshold value for creep management.

Examining the correlation between wheel-slip rate and traction coefficient, Rahaman et al. [9] utilized a dual disc machine to replicate tribological and operational circumstances. The study observes an inverse relationship between traction coefficient and slip rate, with implications for railroad safety and traction control system development.

Zhang et al. [10] explored wheel-rail rolling contact phenomena arising from surface imperfections on individual tracks. The study investigates rolling contact fatigue (RCF) in faulty wheel-rail systems under diverse operating conditions, highlighting the influence of slip ratio and linear velocities on surface damage, fissure depths, and wear debris.

Wang et al. [11] focused on the role of friction modifiers in controlling wheel and locomotive systems. The study uses a twin-disc machine to assess the impact of adhesion and damage behaviours on creepage, wheel/rail contact stress, and FM application. Results indicate promising prospects for FM application in mitigating wheel and rail degradation within specific pressure ranges, elucidating three crucial stages of rail surface fracture propagation.

Additionally, the literatures [12-17] underscore the importance of advanced algorithms, simulation methodologies, and innovative tools in comprehending and mitigating the complex dynamics of wheel-rail interactions.

The research collectively contributes valuable insights to the field, paving the way for enhanced safety, maintenance, and performance in railway systems. There have been valuable insights in the existing literature on rail-wheel interaction complexity, but a research gap is visible in the use of the non-linear Newton-Raphson algorithmic method for determining the characteristics and sensitive regions of the contact zone between rail and wheel. However, previous studies have dwelt on linear analysis with nothing known about non-linear behavior as it affects this vital interface. This lapse requires detailed investigation through non-linear methods in order to understand the complexities of dynamics involved in rail-wheel interactions. Accordingly, this study argues that when we use the nonlinear Newton-Raphson algorithm, new elements will be revealed about structural characteristics and critical regions of the contact zone between the rail and wheel which are currently unknown.

Based on the research gap it is hypothesized that, by using the non-linear Newton-Raphson method of analysis for the rail-wheel contact area, structural features and critical areas that cannot be defined by previous linear and non-linear analyses will be identified in order to enhance understanding of the complexity of the rail-wheel interaction. Laying down the groundwork for the subsequent analysis, the following research questions can be asked:

1- What insights does the non-linear Newton-Raphson algorithm provide on the structural features found in the rail-wheel contact area as oppose to the use of the linear theories?
2- Which of the critical areas in the rail-wheel contact zone have been recognized by the non-linear Newton-Raphson algorithm but cannot be seen by the linear facility?
3- What is the variation between the penetration stress and the frictional stress between linear and non-linear analysis of rail-wheel contact?
4- What are the effects of tread width and tread depth on the structural parameters of the locomotive wheel as calculated based on the results obtained from the response surface optimization?

It is believed that by using this approach, it may be possible to discover some aspects of non-linear behaviour that are missed by traditional linear analyses thereby providing more insight into these two conflicting phenomena. To what extent does the application of the non-linear Newton-Raphson algorithm help us understand structural characteristics and critical regions within rail wheel contact zones better than traditional lines? This study aims to comprehensively assess the structural characteristics and critical zones within the rail-wheel contact region, utilizing the nonlinear Newton-Raphson algorithm. The CAD model of the rail wheel is meticulously developed in ANSYS Design Modeler, and subsequent structural analyses are executed within its static structural analysis system.

2. MATERIALS AND METHODS

2.1 Simulation scheme and geometry

In this study, the dynamic intricacies of locomotive wheel and track interactions are comprehensively explored through the application of the ANSYS program, a robust tool grounded in finite element analysis. The analytical journey unfolds across three pivotal stages: preprocessing, solution, and

postprocessing, each meticulously contributing to the accuracy of our findings. A method based on a KLW data page is applied to find out the ideal locomotive wheel size as depicted in Figure 1.

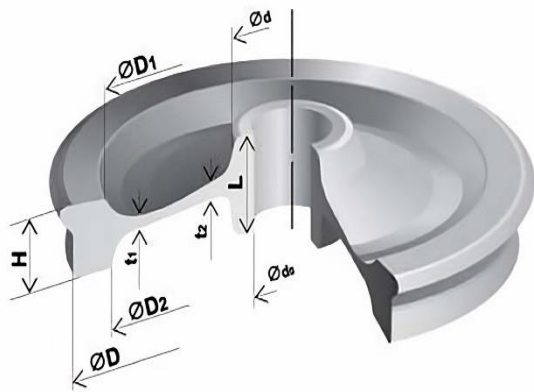| Wheels							
Outside diameter Ø D, mm	Inside Diameter Ø d1 Ø d, mm	Width of rim H, mm	Diameter of hub Ø d, mm	height of hub L,mm	Diameter of hole in hub Ø D₁, mm	Thickness of Disk t₁, t₂, mm	Mass, kg
650-1269	600-1100	95-160	185-500	90-405	60-200	15-80	165-1050

Figure 1. Ideal locomotive wheel size [18]

The material properties are defined for the wheel as EA1N steel which possess good wear resistance, high reliability, high ductility and good thermal resistance, With the help of revolve tool and sketching, this modeling process also includes a rigorous locomotive wheel & track modelling in ANSYS design modeler that we can see as complex 3D CAD vector graphics while approaching Figure 2.
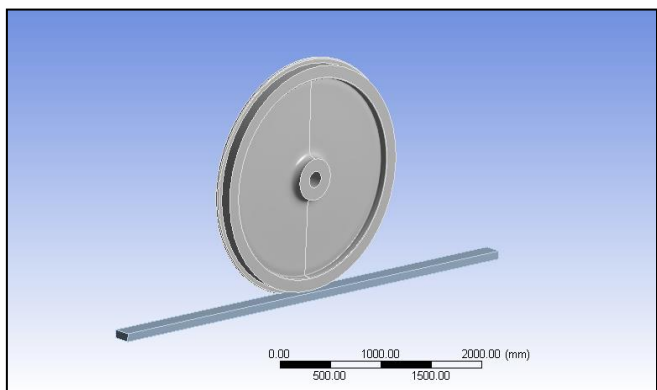

Figure 2. Locomotive wheel and track modelling

2.2 Meshing and analysis consideration

The process of domain meshing is executed using the tetrahedral element type. Tetrahedral elements provide greater freedom of meshing so they are especially good to use for more complex or irregular geometries. This flexibility is crucial to accurately represent the complicated shapes of the locomotive wheel and track system, ensuring that the finite element model sucks up the physical world. It is also possible to utilise computer resources more efficiently, thereby making calculations cheaper without sacrificing the precision of stress and strain forecasts through tetrahedral components. Because of its ability to fabricate curved surfaces more readily, a finer

mesh may be generated in areas that are geometrically complex which results in a fortunate representation between load distribution and stress concentrations [19]. The selection of tetrahedral elements as the preferred option follows from a desire to combine both computational time and accuracy in modeling. Tetrahedral elements allow for increasing the fidelity of our numerical simulations, thus playing a significant role in revealing an accurate and real dynamic behavior we have when analyzing complex systems such as locomotive wheels or tracks where intricate geometries mixed with contact interactions are taking place. The model has a great total of 158,478 components and 251,672 nodes termed as medium which includes diverse features including transition ratios, normalization parameters and inflation settings that are so important in the development of subtle analysis as illustrated below in Figure 3.
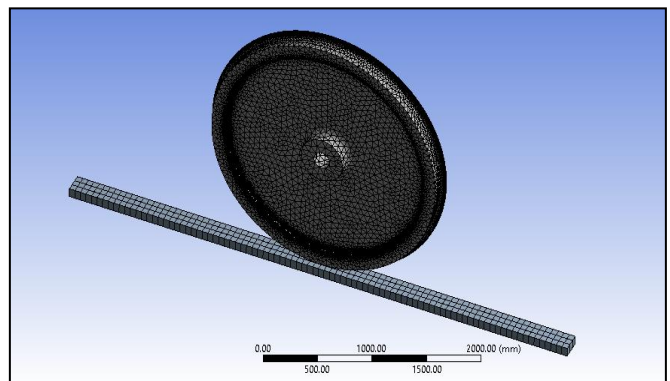

Figure 3. Wheel and track meshed model

Figure 4 depicts the arrangement of a tetrahedral element, consisting of four components, each possessing three degrees of freedom. This representation includes three nodes having 3DOF free i.e., Ux, Uy, and Uz. The contact pair is also generated between the wheel and the track.
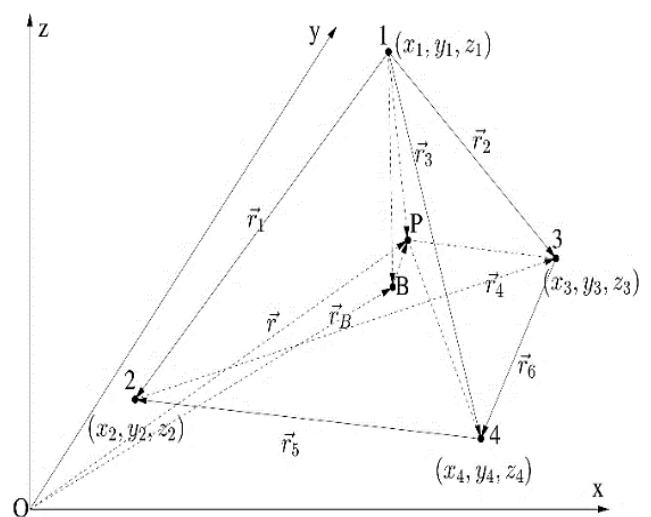

Figure 4. Tetrahedral element shape representation [20]

The narrative transitions to the enactment of contact pairs, specifically the frictional engagement between the locomotive wheel and track, illustrated in Figure 5. A friction coefficient (μ) of 0.25 governs this interaction, while support mechanisms, including a frictionless ally and a fixed support, are strategically positioned.
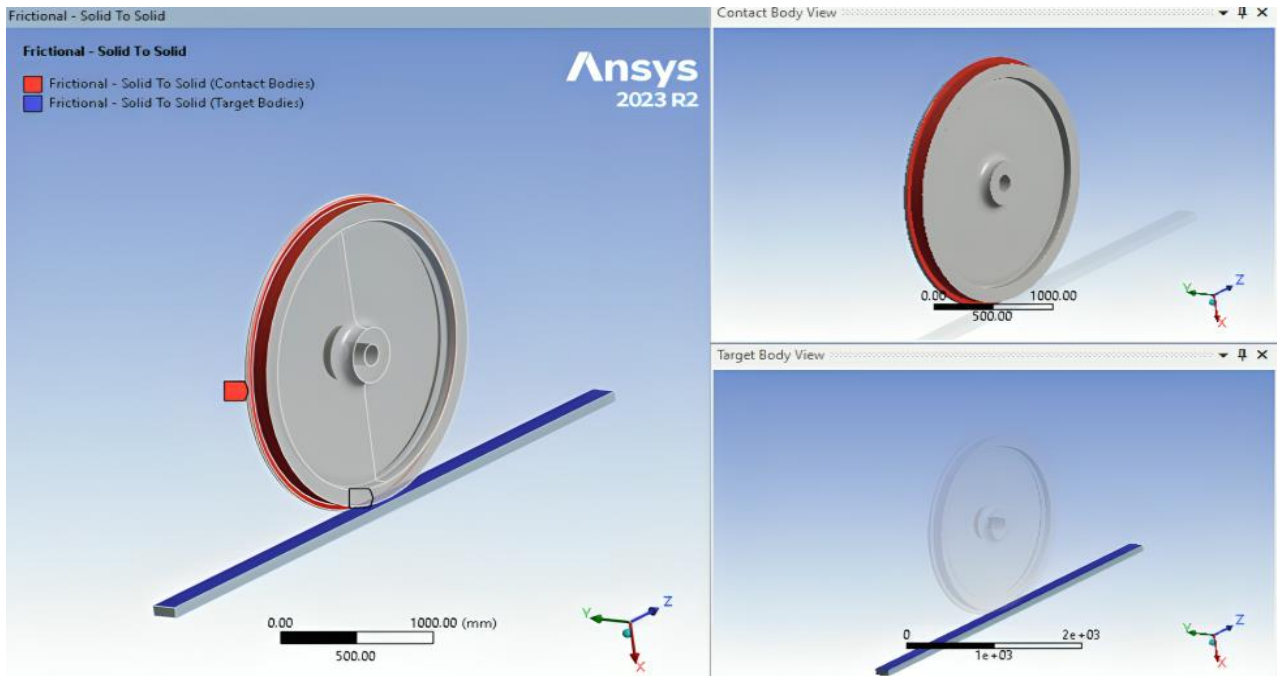
Figure 5. The frictional contact between the wheel and rail

The Newton-Raphson algorithm, adept in handling non-linearity, takes centre stage in the contact pair analysis, depicted geometrically in Table 1.

Table 1. Frictional contact definition

Particular	Details
Frictional coefficient	0.25
Scoping type	Automatic
Contact bodies	Wheel outer surface (red-colored zone)
Target bodies	Track surface (blue-colored zone)

A support with no friction is attached to the side of the wheel, while a support that is fixed is provided to the bottom surface of the track. The inner surface of the hub experiences a vertical force of 146200N. The load and boundary conditions are displayed in Figure 6.
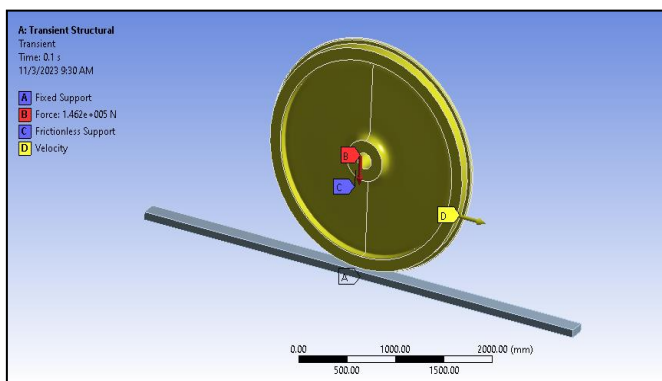

Figure 6. The loads and boundary conditions

Investigating the frictional contact pair involves non-linearity, for which the Newton-Raphson algorithm must be used to find a solution as shown in Figure 7. The solver settings are defined for the simulation. The solver settings include defining load steps which is set to 1, step end time is set to 0.1secs. The auto time stepping is turned OFF with time integration turned ON. For output controls, the stress and strain values are selected. The solver settings are set as program controlled.
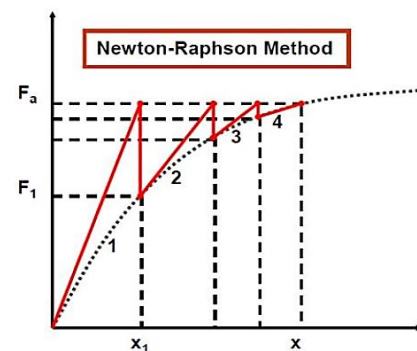

Figure 7. Geometric interpretation of Newton Raphson method (ANSYS solver) [21]

It can be seen from the outset that this methodological symphony as it moves from precise modeling through sophisticated numerics to dynamic friction poses no barrier at all to unravelling wheel/rail interactions of locomotives; on the contrary, it is a fusion of technical prowess and visual allure which makes this complex problem so inherently captivating. The underlying basis for rail engineering's progress in various cyclic creep analyses would seem to be the result not just of the invention but also analysis of pure and simple, writing norms that contribute to track geometry [19]. From preprocessing to postprocessing a painstaking approach suffused with expert know-how ensures a holistic understanding of the behavior of this subtle adversary. Using visually appealing 3D CAD representations, meshing numerical studies, and the inclusion of frictional contact pairs in our work will create a digital platform that realistically mirrors the complex world of rail systems. Using a load and boundary condition array combined with an application of the Newton-Raphson method for nonlinear phenomena would be an important step to take for our contact pair dynamics examination.

3. RESULTS AND DISCUSSION

3.1 Wheel and track contact analysis

In the wheel and track contact analysis, crucial parameters such as equivalent stress, strain, and contact parameters were thoroughly examined. The resulting equivalent elastic strain plot, depicted in Figure 8, highlights a notable elevation in strain within the contact zone.
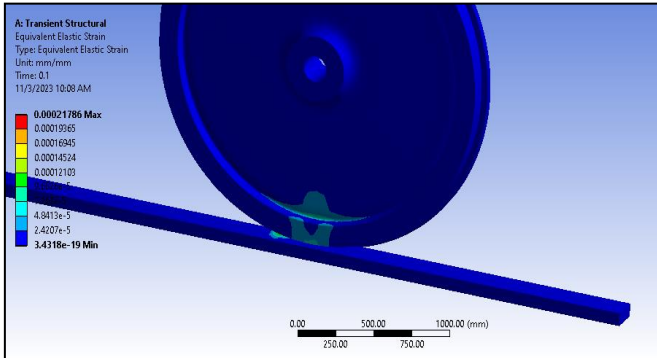

Figure 8. Equivalent elastic strain induced

Meanwhile, the distribution of equivalent stress, illustrated in Figure 9, reveals heightened stress levels concentrated at the inner and bottom faces of the wheel. Remarkably, the obtained stress values exhibit consistency with findings in the existing literature [21].
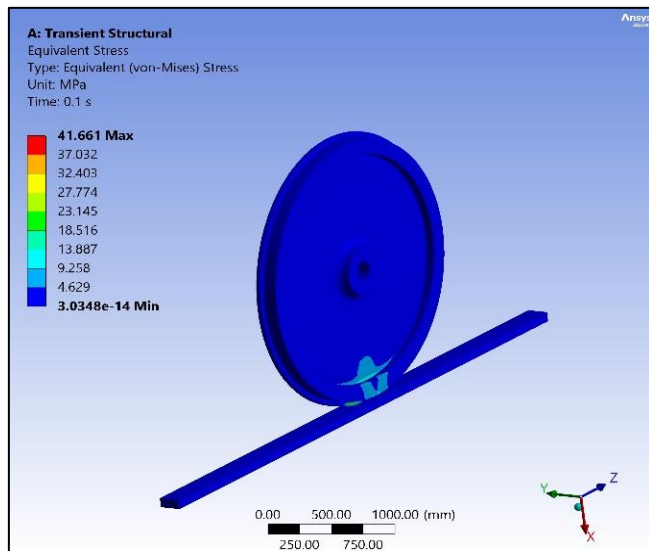

Figure 9. Equivalent stress induced

3.2 Grid refinement

Table 2 presents the outcomes of the grid independence test conducted for the number of elements and equivalent stress (MPa), affirming the reliability and robustness of our analysis.

Table 2. Result of grid independence evaluation

Number of Elements	Equivalent Stress (MPa)
158105	41.619
158335	41.628
158441	41.659
158478	41.661

Figure 10 illustrates the generated contact status for the wheel-rail interaction, unveiling a small region in sliding status amidst predominantly near-contact regions. The outer periphery of the contact zone exhibits a far status, while the inner region portrays a near-contact status, as highlighted in the yellow-colored zone.
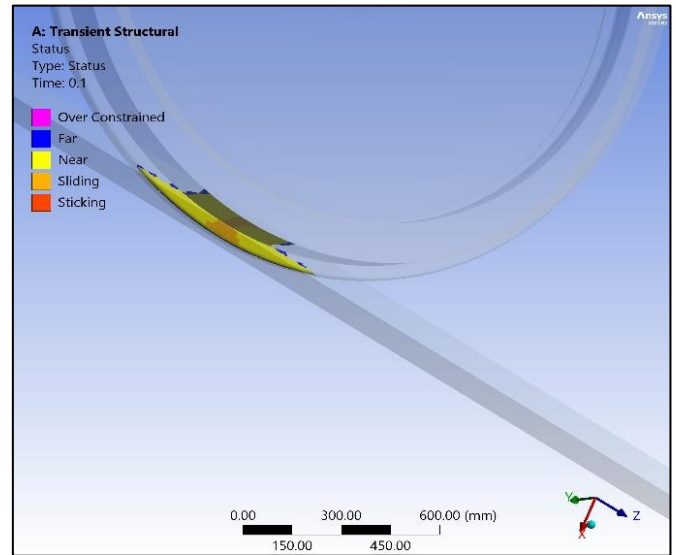

Figure 10. Contact status for the wheel-rail interaction

Complementing this, the frictional stress plot in Figure 11 underscores maximal stress at the sliding zone, gradually diminishing in the near-sliding region. The point of maximum frictional stress aligns with the intersection of the wheel's vertical feature and the rail's horizontal feature.
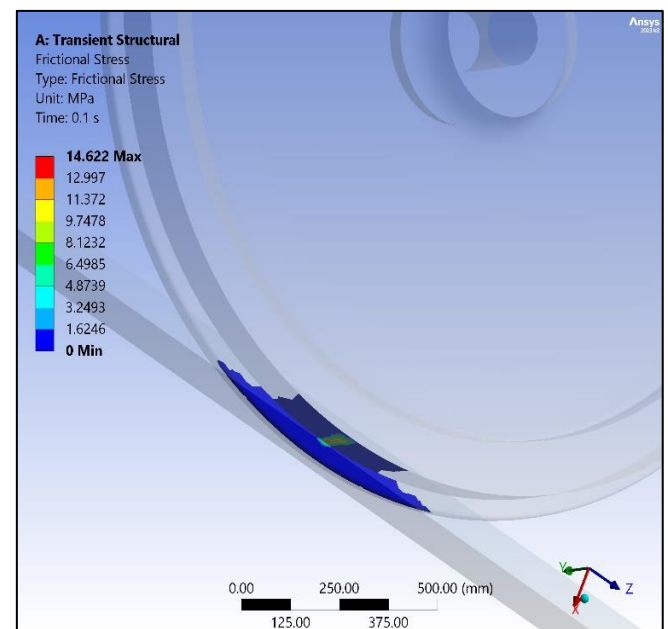

Figure 11. Frictional stress plot

3.3 Contact behavior

For a comprehensive understanding of contact behavior, Figure 12 presents the penetration contour plot for the railway wheel and rail contact region. The analysis reveals that the maximum penetration occurs at the sliding contact zone, with a recorded value of 0.028mm.

A comparative study, detailed in Table 3, contrasts the results between linear and nonlinear analyses. Notably, the findings underscore that linear analysis tends to predict lower penetration values compared to nonlinear analysis, emphasizing the importance of accounting for nonlinearities in such complex interactions.
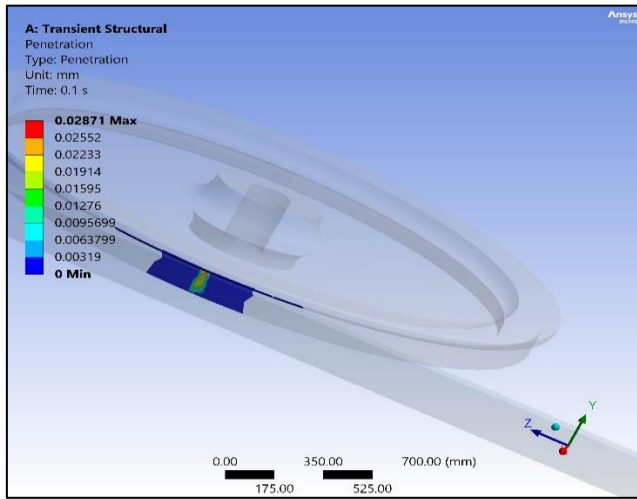

Figure 12. Penetration contour plot for the railway wheel and rail contact region

Table 3. Comparison analysis

Type of Analysis	Contact Status	Penetration (mm)	Frictional Stress (MPa)
Linear Analysis	Small sliding region	0.0215	13.689
Non-Linear Analysis	Small sliding region	0.0287	14.622

The design of the locomotive wheel is then optimized using the optimal space-filling (OSF) algorithm of the response surface optimization method. The design variables are selected for the optimization process i.e. tread_depth and treadwidth as shown in Figure 13. An efficient space-filling scheme offers an important improvement in its capability to spread design points equally so as to obtain an accurate response of the system behavior in all regions as opposed to only a few local areas. The benefit of this feature is that it is essential in the construction of locomotive wheel designs for higher strength and safety factor. This algorithm enables us to place design points intelligently, covering most of design space so that the final design is more robust and plausible.
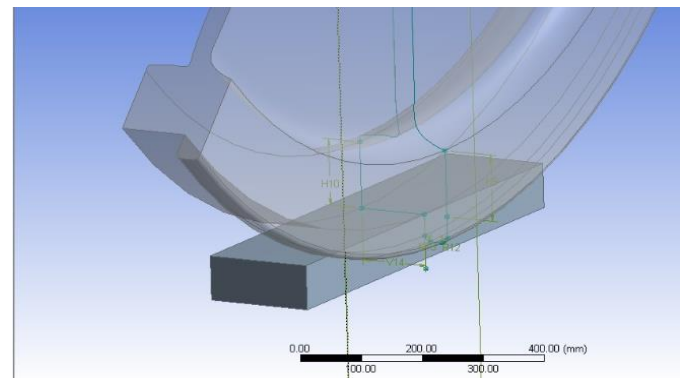

Figure 13. Selection of design variables for optimal space-filling (OSF) algorithm of the response surface optimization

The DOE chart is generated from response surface optimization as shown in Table 4. The variation of tread_depth is shown in column B and the variation of tread_width is shown in column C. Different design points are generated i.e. 1 to 9 as shown in column A. The output parameters for each design point are generated as shown in column D, column E, and column F.

Table 4. Design of experiment chart

Name	P6 tread_depth (mm)	P7 tread_width (mm)	P4 Safety Factor Minimum	P5 Equivalent Stress Maximum (MPa)	P8 Geometry Mass (kg)
1	122.64	112	3.7993	22.689	667.53
2	127.85	117.33	3.4477	25.002	667.27
3	112.2	125.33	2.3031	37,429	682.75
4	120.03	122.67	2.8563	30.179	676.16
5	109.59	109.33	3.8299	22.507	676.11
6	114.81	114.67	3.2261	26.719	675.03
7	117.42	130.67	2.8341	30.415	682.64
8	125.25	128	3.0487	28.274	676.36
9	106.98	120	2.4522	35,152	683.41

The goodness of fit curve is generated for rail wheel optimization as shown in Figure 14. The observed values (as represented by red, green, and blue colored boxes) are in close proximity to the expected values curve (linear straight line) which signifies less deviation and reasonably accurate results.

The variation of safety factor with respect to tread_depth is shown in Figure 15. The safety factor is found to increase linearly with an increase in tread depth. The minimum safety factor is at tread_depth 109mm and the maximum safety factor

is obtained at 130mm.

The variation of safety factor with respect to tread_width is shown in Figure 16. The safety factor is found to decrease with an increase in tread_width. The minimum safety factor is obtained at 125mm tread_width and the maximum safety factor is obtained at 108mm.

The variation of equivalent stress with respect to tread_width is shown in Figure 17. The equivalent stress increases linearly with an increase in tread_width up to

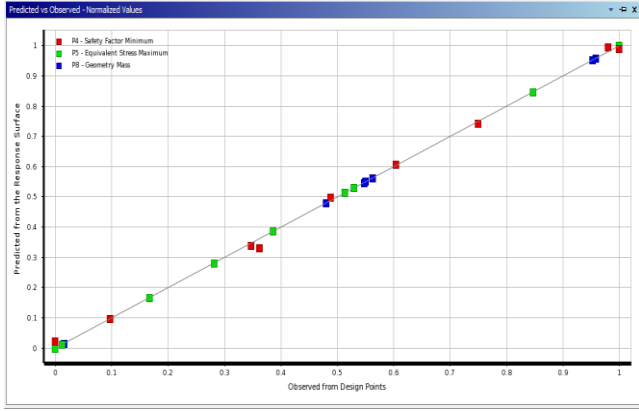126mm and then decreases thereafter. The minimal value of equivalent stress is obtained at 108mm tread_width.

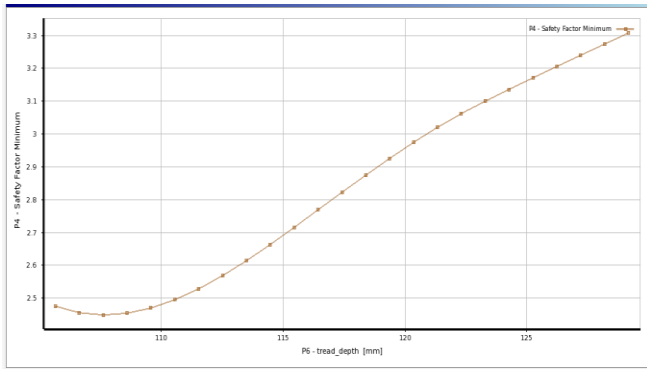

Figure 14. The goodness of fit curve
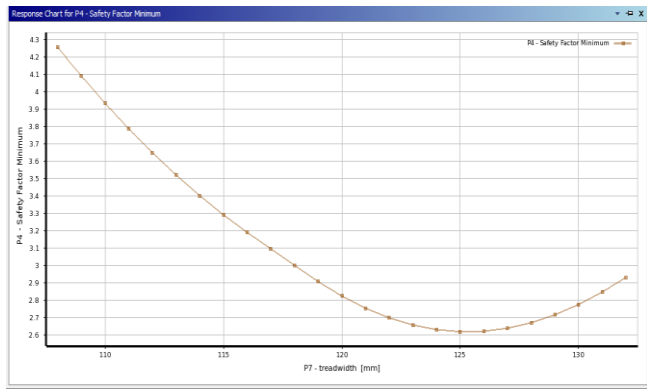

Figure 15. Safety factor vs. tread depth curve

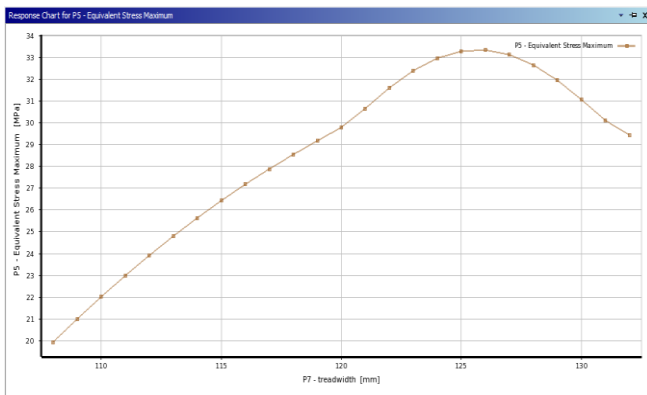**Figure 16.** Safety factor vs. tread_width

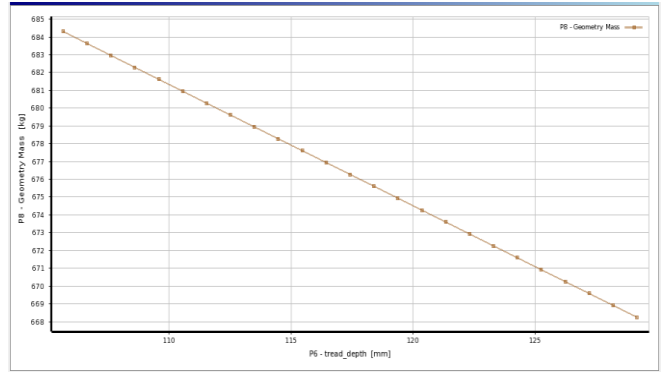**Figure 17.** Equivalent stress vs. tread_width

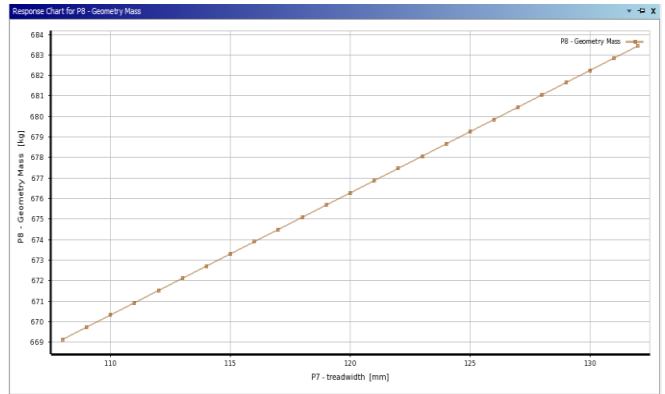**Figure 18.** Mass vs. tread_depth

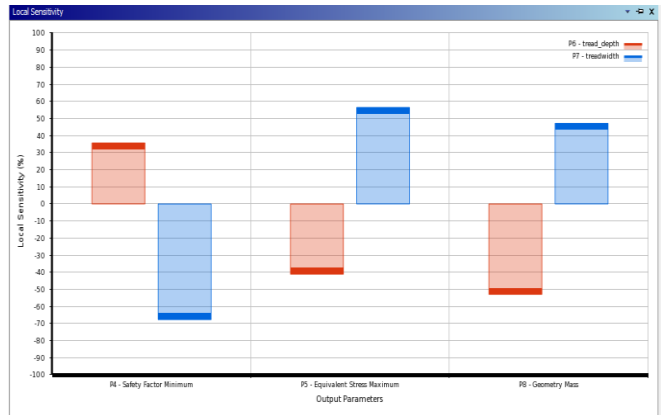**Figure 19.** Mass vs. tread_width

Figure 20. Sensitivity plot

The geometric mass reduces linearly with an increase in tread_depth as shown in Figure 18. The maximum mass is obtained for 104mm tread_depth and the minimum mass is obtained at 129mm tread_depth. The tread_width has a direct effect on the geometric mass of the locomotive wheel (Figure 19). The minimum geometric mass of the locomotive wheel is obtained at 107mm tread_width and the maximum mass is obtained at 133mm.

The sensitivity percentage plot is generated for each design variable of the locomotive wheel as shown in Figure 20. For the safety factor, the tread_width shows a higher sensitivity percentage which signifies that tread_width has a higher effect on the safety factor of the locomotive wheel. For equivalent stress, the tread_width shows higher sensitivity shows higher sensitivity percentage which signifies that tread_width has a higher effect on the induced equivalent stress of the locomotive wheel. For equivalent stress, the tread_width

shows higher sensitivity which signifies that tread_width has a higher effect on the induced equivalent stress of the locomotive wheel. For geometric mass, the tread_depth shows a higher sensitivity percentage as compared to tread_width which signifies that tread_depth has a higher effect on the induced equivalent stress of the locomotive wheel. When the hub width and radius are increased it usually results in stress indicating a greater risk of material fatigue or failure, in high stress situations. However, these adjustments have impact on stress suggesting that the wheels frictional characteristics stay mostly the same. Despite the rise in stress the penetration remains minimal showing that the wheel retains its strength when subjected to the specified loads. It's worth mentioning that a slight increase, in hub width can lead to a mass potentially affecting the locomotives overall weight distribution and dynamic performance.

In summary, careful examination of these data confirms the validity of our approach and offers insightful information about the specifics of wheel-rail contact dynamics. While the differences between linear and nonlinear studies highlight the necessity for a multifaceted strategy in understanding and forecasting the complex behaviors inherent in railway systems, our findings are supported by the literature already in existence. These findings open the door to a deeper understanding of contact mechanics and improved efficiency and safety in rail transportation systems.

4. CONCLUSION

The finite element analysis (FEA) conducted in this study provides valuable insights into the structural dynamics of wheel-rail contact under dynamic loading conditions. We performed a comparative study of linear and nonlinear analyses with a focus on penetration stress as well as frictional race against time. The simulation results vindicate our study hypothesis that the linear analysis, in fact, provides fewer estimates of both penetration and frictional stress than its non-linear form. Although the sliding region is aligned in both analyses, the linear approach always underestimated wheel and rail penetration. For instance, the linear analysis suggested that the penetration value was 25% lower and frictional stress by 6.38% than in the nonlinear one. The response surface optimization process is conducted on the locomotive wheel to evaluate the effect of tread_width and tread_depth on structural parameters. The optimization technique employed would serve as guidance in improving the design of the locomotive wheel. To summarize the findings:

1. Insight from non-linear analysis: The non-linear Newton-Raphson algorithm would provide a better estimate of penetration and frictional stress compared to linear analysis. In contrast, penetration was underestimated by 25% by the linear analysis and frictional stress was underestimated by 6.38%.

2. Non-linear critical regions: Critical regions on the rail-wheel contact pair in the non-linear analysis are identified. This emphasises the ability of the non-linear approach to identify previously undescribed areas of importance to the interaction dynamics.

3. Variances in stress values: The evaluation of differences of Penetration stress and Frictional stress between linear and non-linear approaches and how much they differ, was considerable. These detailed stress distributions showed the need for advanced analytical techniques for a comprehensive understanding of rail-wheel interactions as the linear and non-

linear analysis of the cantilever rail specimen delivered a higher resolution and accuracy of stress fields.

4. The impact of tread dimensions on response surface optimization: Response surface optimization showed that tread width and tread depth have a strong effect on locomotive wheel mechanical characteristics. The analysis above highlights the significance of them in railway systems design, construction and maintenance, which offers engineering references.

Although our study illuminated the limitations of linear analysis when trying to understand the complexities of wheel-rail contact, we must recognize several limitations within our methodology. Maybe there are other factors in real-world situations that our simulation would not be able to fully reflect. The accuracy of our predictions could be affected by the variability in material properties, environmental conditions, or track irregularities. The potential for future exploration and improvement is huge. Future studies may focus on the incorporation of advanced material models that can consider the complex behaviors of railway components under different circumstances.

Furthermore, the incorporation of real-world data and field observations into our simulations could enhance the accuracy and relevance of our findings. In other words, the study has helped deepen understanding of wheel-rail contact dynamics, highlighting nonlinear analysis as crucial in capturing all subtle intricacies that are typical for real-life situations. Addressing the shortcomings of linear analysis would open doors to more precise predictions and better design theories related to rail transportation systems.

REFERENCES

[1] Wen, Z., Jin, X., Xiao, X., Zhou, Z. (2008). Effect of a scratch on curved rail on initiation and evolution of plastic deformation induced rail corrugation. International Journal of Solids and Structures, 45(7-8): 2077-2096. https://doi.org/10.1016/j.ijsolstr.2007.11.013

[2] Ling, L., Cao, Y.B., Xiao, X.B., Wen, Z.F., Jin, X.S. (2015). Effect of wheel flats on the high-speed wheel-rail contact behavior. Journal of the China Railway Society, 37: 32-39. https://doi.org/10.3969/j.issn.1001-8361.2015.07.006

[3] Wen, Z., Jin, X., Zhang, W. (2005). Contact-impact stress analysis of rail joint region using the dynamic finite element method. Wear, 258(7-8): 1301-1309. https://doi.org/10.1016/j.wear.2004.03.040

[4] Zhou, X., Zhao, X., Han, J., He, Y.P., Wen, Z.F., Jin, X.S. (2018). Study on transient rolling noise characteristics of subway wheel with rail corrugation. Journal of Mechanical Engineering, 54(4): 196-202. https://doi.org/10.3901/JME.2018.04.196

[5] Chang, C., Chen, B., Liang, H. (2021). Experimental study on traction adhesion coefficient between wheel and rail in water condition within 400 km/h speed grade. China Railway Science, 42: 132-137.

[6] Spiryagin, M., Bernal, E., Oldknow, K., Persson, I., Rahaman, M.L., Ahmad, S., Wu, Q., Cole, C., Mcsweeney, T. (2023). Implementation of roughness and elastic-plastic behavior in a wheel-rail contact modeling for locomotive traction studies. Wear, 532: 205115. https://doi.org/10.1016/j.wear.2023.205115

[7] Bernal, E., Spiryagin, M., Vollebregt, E., Oldknow, K., Stichel, S., Shrestha, S., Ahmad, S., Wu, Q., Sun, Y., Cole, C. (2022). Prediction of rail surface damage in locomotive traction operations using laboratory-field measured and calibrated data. Engineering Failure Analysis, 135: 106165. https://doi.org/10.1016/j.engfailanal.2022.106165

[8] Tao, G., Wen, Z., Guan, Q., Zhao, X., Luo, Y., Jin, X. (2019). Locomotive wheel wear simulation in complex environment of wheel-rail interface. Wear, 430: 214-221. https://doi.org/10.1016/j.wear.2019.05.012

[9] Rahaman, M.L., Bernal, E., Spiryagin, M., Bosomworth, C., Sneath, B., Wu, Q., Cole, C., McSweeney, T. (2023). An investigation into the effect of slip rate on the traction coefficient behaviour with a laboratory replication of a locomotive wheel rolling/sliding along a railway track. Tribology International, 187: 108773. https://doi.org/10.1016/j.triboint.2023.108773

[10] Zhang, S.Y., Ding, H.H., Lin, Q., Liu, Q.Y., Spiryagin, M., Wu, Q., Wang, W.J., Zhou, Z.R. (2023). Experimental study on wheel-rail rolling contact fatigue damage starting from surface defects under various operational conditions. Tribology International, 181: 108324. https://doi.org/10.1016/j.triboint.2023.108324

[11] Wang, W., Li, S., Ding, H., Lin, Q., Galas, R., Omasta, M., Meli, E., Guo, J., Liu, Q. (2023). Wheel/rail adhesion and damage under different contact conditions and application parameters of friction modifier. Wear, 523: 204870. https://doi.org/10.1016/j.wear.2023.204870

[12] Chen, C., Wei, L., Chen, Z., Guo, C. (2019). Operation planning for freight block trains using released transport capacity of existing railways. Journal Européen des Systèmes Automatisés, 52(5): 495-500. https://doi.org/10.18280/jesa.520508

[13] Agarwal, A., Mthembu, L. (2023). FE structural analysis and experimental investigation of HMV chassis. In Emerging Trends in Mechanical and Industrial Engineering: Select Proceedings of ICETMIE 2022, Singapore, Springer Nature, pp. 931-943. https://doi.org/10.1007/978-981-19-6945-4_70

[14] Agarwal, A., Batista, R.C. (2023). CFD analysis of flow behavior and thermal performance in single and multi-inlet EGR coolers. International Journal of Heat and Technology, 41(3): 673-678. https://doi.org/10.18280/ijht.410320

[15] Agarwal, A., Batista, R.C., Tashi, T. (2024). Crashworthiness evaluation of electric vehicle battery packs using honeycomb structures and explicit dynamic analysis. In E3S Web of Conferences, EDP Sciences, 519: 04010. https://doi.org/10.1051/e3sconf/202451904010

[16] Wu, M.L., Lu, Z., Chun, T. (2017). Modelling and simulation of complex pneumatic control valve for train braking systems. International Journal of Transport Development and Integration, 2(2): 202-214. https://doi.org/10.2495/TDI-V2-N2-202-214

[17] Trulli, E., Rada, E.C., Conti, F., Ferronato, N., Raboni, M., Talamona, L., Torretta, V. (2018). Fire simulation in a full-scale bilevel rail car: Experimental analysis to assess passenger safety. International Journal of Safety and Security Engineering, 2018(1): 110-120. https://doi.org/10.2495/SAFE-V8-N1-110-120

[18] Lal, H., Singh, B. (2020). Design optimization for weight reduction of locomotive wheel using response surface methodology. International Journal of Engineering Technologies and Management Research, 6: 39-46. https://doi.org/10.29121/ijetmr.v6.i1.2019.344

[19] Fedorko, G., Molnár, V., Blaho, P., Gašparík, J., Zitrický, V. (2020). Failure analysis of cyclic damage to a railway rail – A case study. Engineering Failure Analysis, 116: 104732. https://doi.org/10.1016/j.engfailanal.2020.104732

[20] Nentchev, A. (2008). Numerical analysis and simulation in microelectronics by Vector Finite Elements Dissertation, Technische Universität Wien. https://doi.org/10.34726/hss.2008.10738

[21] Gennaro. (2019). Evaluation of stiffness matrix at iteration ith – Newton-Raphson method. In ANSYS General Mechanical. https://forum.ansys.com/forums/topic/evaluation-of-stiffness-matrix-at-iteration-ith-newton-raphson-method/, accessed on 12 Feb. 2023.